

# ROLLING TEXTURES OF A CU-20%NB COMPOSITE

D.Raabe, J.Ball, G.Gottstein

Institut für Metallkunde und Metallphysik, Kopernikusstr.14, 5100 Aachen, Germany

(Received March 24, 1992)

(Revised May 18, 1992)

## Introduction

Copper and Niobium have no mutual solubility by practical standards. Therefore, fibre or ribbon reinforced in-situ MMCs can be produced by large degrees of deformation, e.g. by wire drawing or rolling of a cast ingot. The Cu-20 vol% Nb composite has been under intensive investigation in the past owing to the high tensile strength of the deformed material, actually much higher than expected from the rule of mixtures of the component strength [1-5]. Several models have been proposed to explain the observed strength anomaly. The barrier model by Spitzig and coworkers [1-3,6,7] attributes the strength to the difficulty of propagating plastic flow through the fcc-bcc interfaces while the group of Courtney and coworkers interprets the strength in terms of geometrically necessary dislocations owing to the incompatibility of plastic deformation of the bcc and fcc phase [5]. In fact both models are able to describe the observed increase of strength by assumption of reasonable fitting parameters. However, the actual structure evolution and strengthening processes are still unknown.

This investigation is concerned with the texture development by rolling of Cu 20% Nb. The crystallographic texture is of interest for three reasons in this context. Firstly, the texture can be very sensitive to the deformation process and microstructure evolution [12]. Secondly, the orientation distribution affects the strength of the material in terms of the Taylor factor [9-11]. Thirdly, the influence of a massive second phase on texture development is of general interest for texture evolution of in-situ mechanically processed composites.

## Experimental

The initial Cu-20 vol% Nb ingot of  $100 \cdot 50 \cdot 25 \text{ mm}^3$  was prepared in a vacuum induction furnace. A sample of  $50 \cdot 24 \cdot 22 \text{ mm}^3$  was machined from the cast ingot and rolled to  $\epsilon=60\%$  on a two-high mill with an initial roll diameter of 250mm, followed by 60mm and finally 30mm. This sequence of roll diameters was chosen to obtain homogeneous deformation, which is primarily determined by the ratio of contact length to specimen thickness  $l_c/d$ . After rolling degrees of  $\epsilon=88\%$ , 96%, 97%, 99% and 99.5% samples were prepared for texture measurements near the surface and in the center layer. The same rolling procedure was also applied to single phase Nb specimens. For texture measurements the samples were etched in a solution of 10ml  $\text{CH}_3\text{COOH}$ , 3 ml  $\text{HNO}_3$  and 1 ml HF to remove a surface layer of at least  $20 \cdot 10^{-6} \text{ m}$ . Incomplete x-ray pole figures were measured from an area of  $14 \cdot 24 \text{ mm}^2$  in the range of the poledistance angle  $\alpha$  from  $5^\circ$  to  $\alpha=85^\circ$  by means of a fully automatic texture goniometer in the back reflection mode [12,13,19]. From a set of four incomplete pole figures ( $\{111\}$ ,  $\{200\}$ ,  $\{220\}$ ,  $\{311\}$  for Cu and  $\{110\}$ ,  $\{200\}$ ,  $\{112\}$ ,  $\{103\}$  for Nb) the orientation distribution function (ODF) was calculated using the series expansion method to  $l_{\text{max}}=22$  [19]. For "ghost" correction and elimination of truncation errors the calculated ODFs were approximated by model ODFs [20,21].

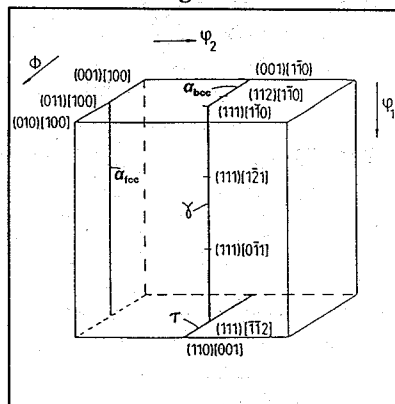


Fig.1  
Definition of fibres in reduced Eulerspace

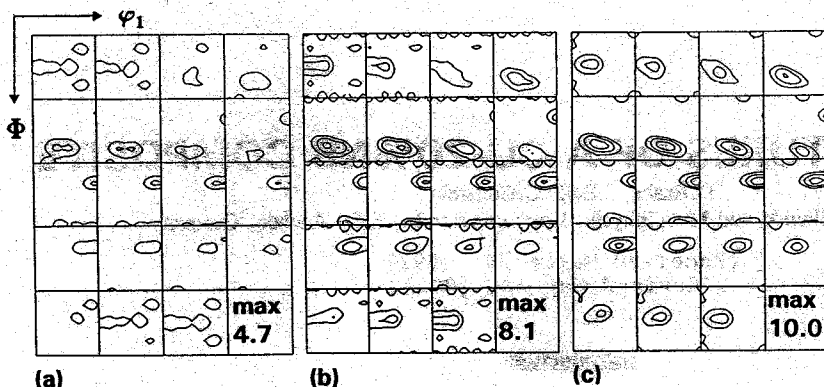


Fig. 2a-c

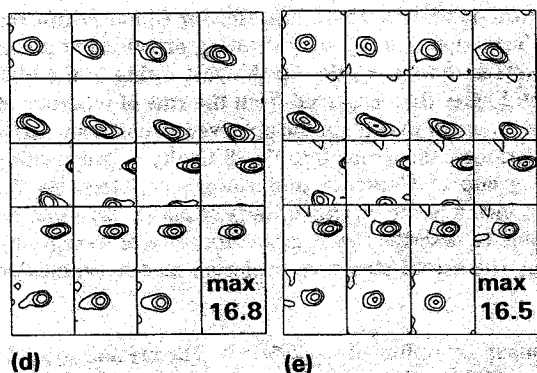


Fig. 2d,e

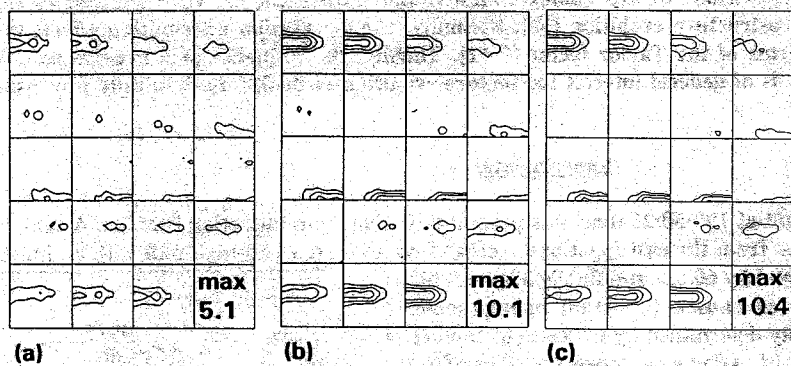


Fig. 3a-c

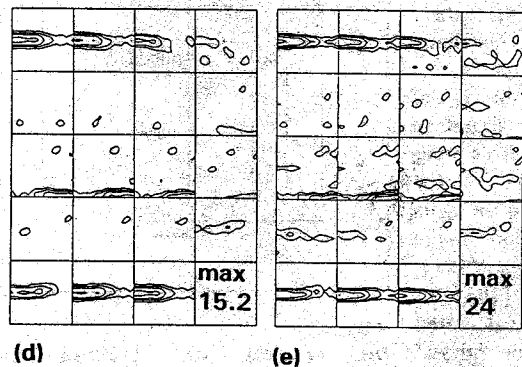


Fig. 3d,e

Results and Discussion

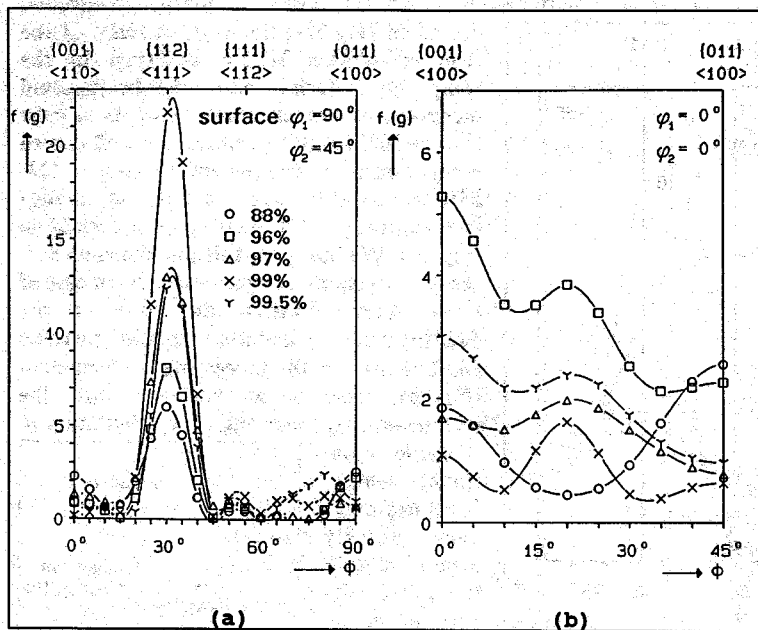


Fig.4 Cu in the composite, (a)  $\tau$ -fibre, (b) Cube RD rotation

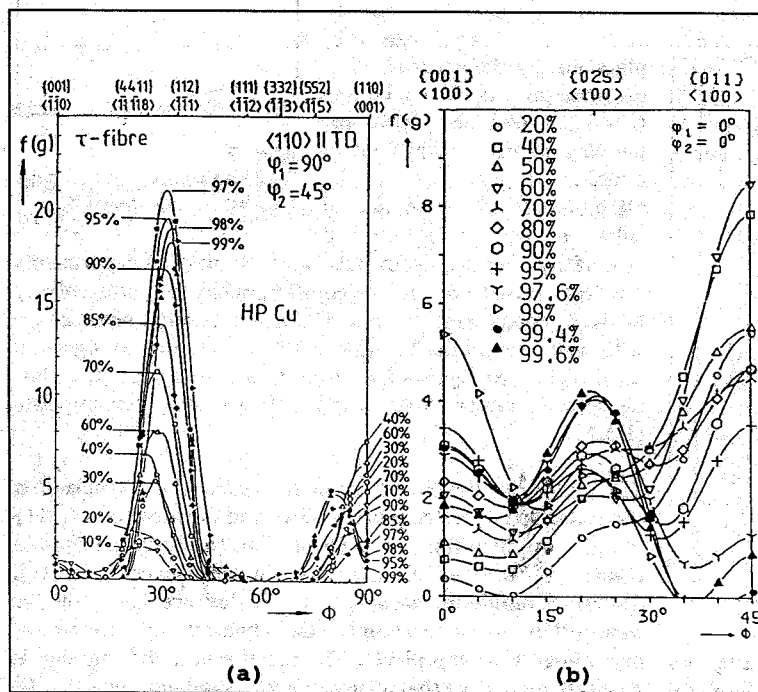


Fig.5 Single phase Cu, (a)  $\tau$ -fibre (b) Cube Rd rotation

The rolling textures of Cu and Nb in the Cu-20% Nb composite are shown in Figs. 2 and 3, although not in a traditional representation. Orientation distributions are conventionally represented in terms of Euler angles  $\varphi_1$ ,  $\Phi$  and  $\varphi_2$  in the reduced Euler space, which is depicted in Fig.1 [19]. Commonly, for ODF representation of fcc metals like Cu, sections of  $\varphi_2 = \text{constant}$  are used, whereas for bcc metals like Nb, sections of  $\varphi_1 = \text{constant}$  are preferred [12,15-18]. To achieve a better comparison of both types of textures in this study, the Nb ODFs are rotated 90° about the transverse direction and are also presented in sections of  $\varphi_2 = \text{constant}$ . This is because of the reciprocity of slip plane and slip direction in fcc and bcc crystals respectively:  $\{hkl\}_{fcc} = \langle uvw \rangle_{bcc}$  and  $\langle uvw \rangle_{fcc} = \{hkl\}_{bcc}$ . This correspondence is equivalent to a rotation of 90° about the transverse direction [22].

The ODFs of Cu and Nb, respectively, in the composite sample remain similar with increasing degree of rolling, but there are noticeable changes of intensity. This can best be seen from the intensity distribution along certain lines in Euler space, the so called fibres, which are defined in Fig.1. The rolling texture evolution of Cu in the composite (Figs.2a-e,4a,b) is very similar to the texture development of pure Cu [12], except for two details. At very large deformation ( $\epsilon = 99.5\%$ ) the C orientation  $\{112\} \langle 111 \rangle$  decreases from 16 vol% to 10 vol%, whereas the random component (background) rises from 20 vol% to 26 vol%. From measurements on pure

Cu it is well known, that the C component decreases at very large deformation, while the twin of first generation of the C orientation, which can be found on the  $\tau$ -fibre at  $\Phi=75^\circ$ , increases and the background decreases (Fig.5a). Such an increase of the twin orientation is not observed in the composite material. Also, the background increases. Moreover, small amounts of cube texture  $\{001\} \langle 100 \rangle$ , which is a well known recrystallization component in copper [23-25], appear (Figs.2a-e), but do not change systematically with increasing deformation (Fig.4b). We interpret this phenomenon as a result of dynamic recrystallization. In case of static recrystallization the cube or the  $\{025\} \langle 100 \rangle$  orientation should increase continuously with increasing deformation (Fig.5b). This is at variance with the measurements. Since the cube orientation is unstable upon further rolling, it rotates away very quickly around  $\Phi$  with increasing degree of deformation, so that no steady increase of the cube component can take

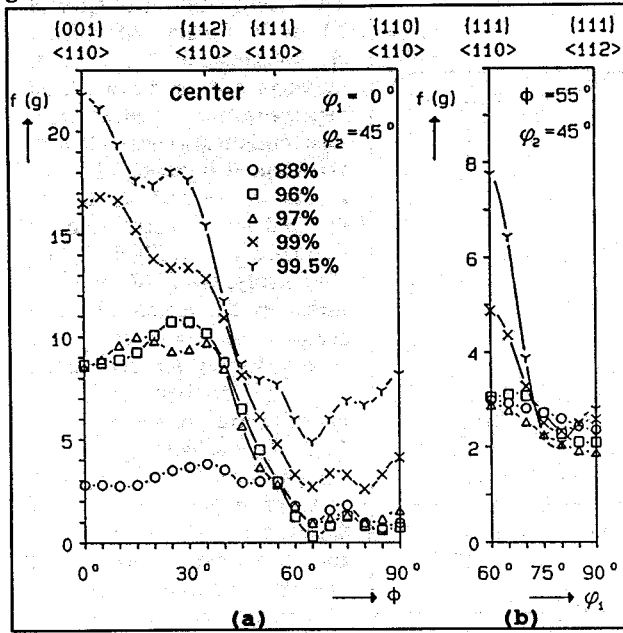


Fig. 6 Nb in the composite, (a)  $\alpha_{bcc}$ -fibre, (b)  $\gamma$ -fibre

place during deformation. The decrease of the C orientation (Fig.4a), combined with the increase of the background at  $\epsilon=99.5\%$  can then be attributed to the formation of cube nuclei from the C orientation, because from static recrystallization experiments it is known that the cube orientation nucleates preferentially in the C component [23-25]. The newly formed orientations with volume fractions below 2-3% enrich the background only. This interpretation would also explain the low dislocation density observed in the Cu phase of the composite [1-3,28].

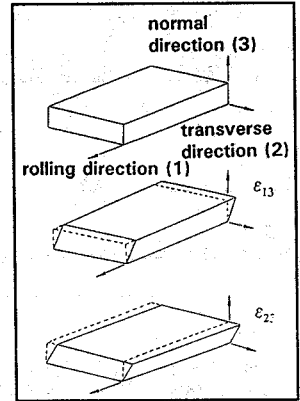


Fig. 7 Definition of the shear components

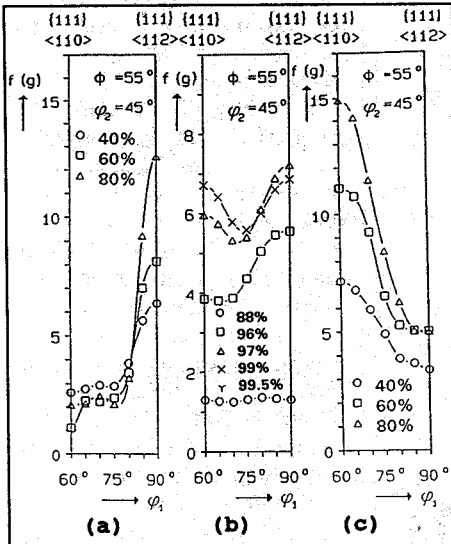


Fig. 8 Simulated textures according to relaxed constraints Taylor theory, with relaxation of (a)  $\epsilon_{13}$  (b)  $\epsilon_{13}$  and  $\epsilon_{23}$  (c)  $\epsilon_{23}$

The texture of the Nb phase in the composite (Figs.3a-e) is characterized by a sharp bcc- $\alpha$ -fibre and the absence of  $\{111\} \langle 112 \rangle$  on the  $\gamma$ -fibre (Figs.6a,b). This can be understood in terms of "Relaxed Constraints Taylor Theory" [10,11]. Texture simulations according to Taylor are based on the description of macroscopic deformation by means of crystallographic slip [9-11]. The macroscopic deformation is characterized by the displacement gradient tensor. Its symmetric part represents the strain tensor, while the antisymmetric part describes the resulting rigid body rotation. The macroscopic deformation during rolling consists of elongation in rolling direction and thickness reduction

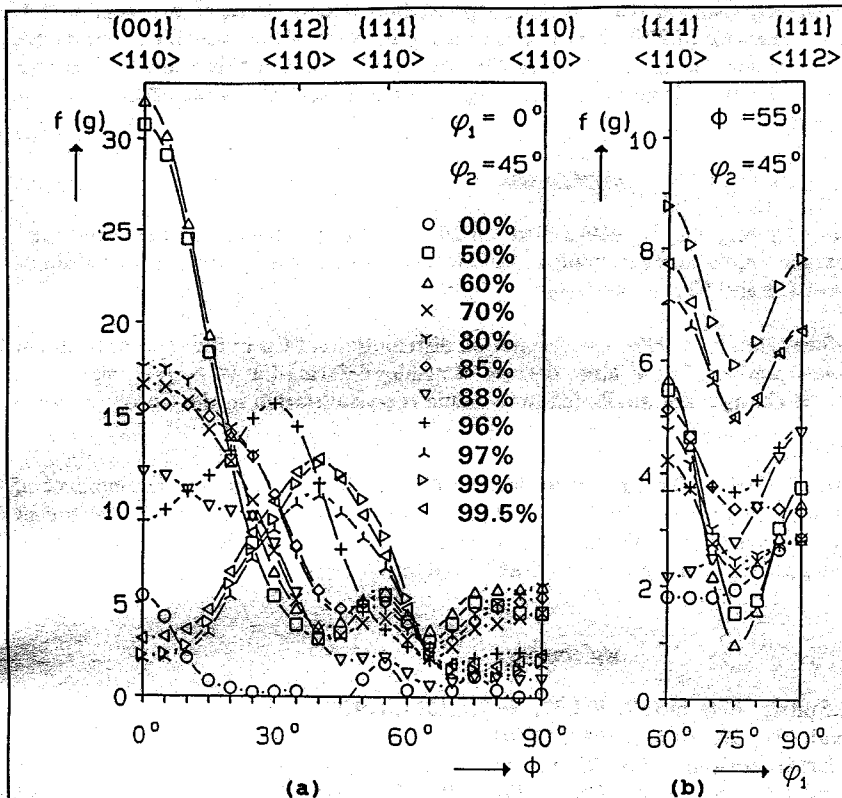


Fig. 9 Single phase Nb, (a)  $\alpha_{bcc}$ -fibre (b)  $\gamma$ -fibre

parallel to the sheet plane normal, but no shears are involved. The relaxed constraints Taylor theory assumes also shear strains to occur microscopically, i.e. relaxes the zero shear constraints locally. A relaxation of the strain component  $\epsilon_{13}$  corresponds to a shear in longitudinal direction, while  $\epsilon_{23}$  denotes the shear in transverse direction (Fig.7). Allowing for these shears locally leads to distinct changes in the rigid body rotation and thus in the texture development when compared to the predictions by full constraints Taylor theory [9-12,22]. The Nb texture in the composite can successfully be modelled by Taylor theory with relaxed  $\epsilon_{23}$  constraints (Fig.6b,8c). For single

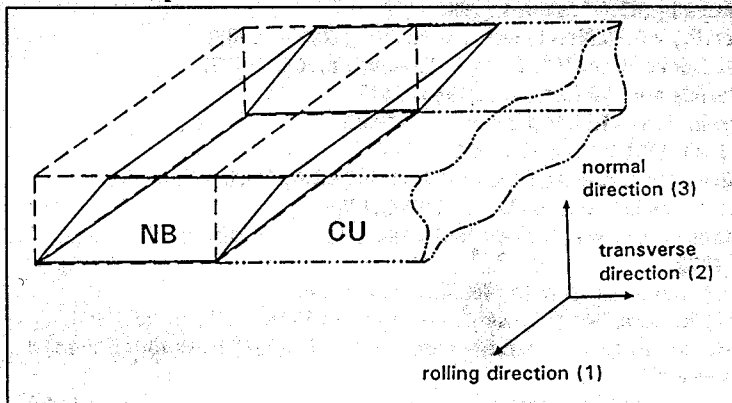


Fig. 10 Illustration for transverse shear of Nb in Cu Nb composite

phase material the  $\epsilon_{13}$  and the  $\epsilon_{23}$  constraints both can be relaxed because of microstructure evolution during deformation ("pancake-model"). The simulated texture shown in Fig.8b corresponds very well to the measurements of pure Nb (Fig.9b). Relaxation of the  $\epsilon_{13}$  shear (Fig.8a) or both  $\epsilon_{13}$  and  $\epsilon_{23}$  shear (Fig.8b) leads to a strong  $\{111\} \langle 112 \rangle$  texture component, which is typical for single phase bcc metals like pure Nb (Fig.9b), [17]. In single phase material, however, a significant shear  $\epsilon_{23}$  cannot be allowed without generating severe incompatibility problems between adjacent grains. In a composite, however, the Nb ribbons are embedded in a softer, maybe even recrystallized Cu matrix, which mitigates the incompatibility created by a shear  $\epsilon_{23}$  in the Nb (Fig.10). Allowing for  $\epsilon_{23} \neq 0$

during rolling, suppresses the development of the  $\{111\} \langle 112 \rangle$  component (Fig.8c) in agreement with the Nb texture in the composite (Fig.6b). This means that in the composite the constraints for Nb become

anisotropic, allowing a stronger  $\epsilon_{23}$  shear of Nb into the Cu phase but hinders its  $\epsilon_{13}$  shear. Finally, it is noted that at degrees of rolling in excess of 97% there is also a strong increase of the rotated cube in the Nb phase of the composite (Fig.6a at  $\Phi=0^\circ$ ), but not in pure Nb. The development of this component cannot be explained by simple deformation models and has to be subject to more detailed investigations.

### Conclusions

The crystallographic texture of a very heavily cold rolled Cu-20 vol% Nb composite was measured. The results were compared to texture simulations according to Taylor theory and to the rolling textures of single phase polycrystalline sheets of Cu and Nb, respectively.

At low and intermediate deformation ( $\epsilon < 99\%$ ) the orientation distributions of Cu in the composite and of single phase Cu developed very similar but at large degrees of rolling deformation ( $\epsilon \geq 99\%$ ) significant differences were observed. The changes are attributed to dynamic recrystallization in the Cu phase of the composite.

The textures of Nb in pure Nb and in the composite develop differently such that the development of  $\{111\} <112>$  is suppressed in the composite. This behaviour can be successfully modelled by Taylor theory with relaxed  $\epsilon_{23}$  and enforced  $\epsilon_{13}$  constraints. We propose to interpret this unusual transverse shear as the consequence of the embedding of hard Nb ribbons in a soft Cu matrix.

### References

1. C.L.Trybus and W.A.Spitzig, Acta metall. Vol.37, Nr.7,p.1971, (1989)
2. W.A.Spitzig, Acta metall. Vol.39, Nr.6, p.1085, (1991)
3. W.A.Spitzig and P.D.Krotz, Scripta metall. 21, p.1143, (1987)
4. J.Bevk.,J.P.Harison and J.L.Bell, Journ. of appl. Phys. 49, p.6031, (1978)
5. P.D.Funkenbusch and T.H.Courtney, Acta metall. 33, p.913, (1985)
6. J.C.Li and Y.Chou, Metall. trans.1, p.1145, (1970)
7. J.C.Li, Trans. Amer. Inst. Min. Eng. 227, p.239, (1963)
8. M.F.Ashby, Strength. Methods in Crystals, p.137, Wiley, New York, (1971)
9. G.I.Taylor, Journal inst. met.62, p.307, (1938),
10. R.Fortunier,J.Hirsch in "Theor. techniques of texture analysis" ed. by H.J.Bunge,DGM Verlag (1986)
11. J.F.W.Bishop and R.Hill, Philos. mag.,42,(1951),414,1298
12. J.Hirsch and K.Lücke, Acta metall., vol.36,Nr.11,overview Nr.76, p.2863, (1988)
13. J.Hirsch,M.Loock,L.Loof and K.Lücke,Proc. ICOTOM 7, Holland, p.765, (1977)
14. H.Mecking in "Strength of Materials and Alloys",vol.3,(1980),1573
15. K.Lücke,C.Därmann and J.Hirsch, Trans.Ind.Met.38, p.496, (1985)
16. M.Hölscher and K.Lücke,Proc ICOTOM 9,France, p.585, (1990)
17. M.Hölscher, D.Raabe and K.Lücke, steel research 12, p.567, (1991),ed.by Verlag Stahleisen
18. U.v.Schlippenbach,F.Emren and K.Lücke, Acta metall.34,(1986),1289
19. H.J.Bunge,"Mathematical Methods of Texture Analysis",Akademie Verlag Berlin, pp.20, (1969)
20. S.Matthies,Phys.stat.sol.(b) 92,(1979),35
21. K.Lücke,J.Pospiech,K.H.Viernich and A.Jura, Acta metall.29,(1981),167
22. M.Hölscher, Dissertation, RWTH Aachen,"Roll. and Recryst. Text. of Fe16%Cr", p.115, (1987)
23. H.Hu,"Recr.,Grain Growth", ed. N.Hansen and D.Juul-Jensen, Proc. 7. RISO Roskilde,Denmark
24. I.L.Dillamore,H.Katoh, Met.Science 8,(1974),73
25. H.Hu, "Text. in Res. and Practise", ed.by J.Grewen,G.Wassermann, Springer Verlag Berlin,(1969)
26. G.Langford and M.Cohen, Trans. of ASM, Vol.62, p.623, (1969)
27. W.F.Hosford,jr., Trans. of TMS AIME, Vol. 230, p.12, Febr. 1964
28. E.Weidmann, Diploma thesis, RWTH Aachen, p.8, 1991
29. H.Hammelrath, Dissertation, RWTH Aachen,"Devel. of Roll. and Recr. Tex. in Cu", p.I-33, (1990)